

(Supplementary data file)

In-Situ Polypyrrole Coating on Copper Foam via Femtosecond laser-Irradiation for supercapacitor applications

Muhammad Faheem Maqsood^{1,*}, Faisal Ghafoor², Syed Muhammad Zain Mehdi^{1,3}, Iqra Rabani^{1,4*}

¹Department of Nanotechnology and Advanced Materials Engineering, Sejong University, Seoul 05006, South Korea

²Department of Electrical Engineering, Sejong University, Seoul 05006, Republic of Korea

³School of Chemical, Biological and Battery Engineering, Gachon University, 1342 Seongnam-daero, Sujeong-gu, Seongnam-si, Gyeonggi-do 13120, Republic of Korea

⁴Antwerp engineering, photoelectrochemistry and sensing (A-PECS), University of Antwerp, Groenenborgerlaan 171, 2020 Antwerp, Belgium

*email: faheem@sju.ac.kr (M.F Maqsood), Iqra.rabani@uantwerpen.be (I. Rabani)

2.1 Materials

Copper (Cu) foam (purity > 99%) of 1 mm thickness was sourced from Tmax Battery Equipment Ltd. (China). Analytical grade potassium hydroxide (KOH) and Pyrrole (C₄H₅N) were acquired from Sigma-Aldrich (USA).

2.2 Preparation of electrode

Detailed descriptions of the Fs laser treatment process can be found in previous work [1, 2]. However, in this study, the laser parameters were set to a power of 2 W, a scanning speed of 20 mm/s, and a pulse duration of 20 femtoseconds, with a 0.04 mm spacing between irradiation points on the Cu foam, producing the final binder free polypyrrole (PPy) coated Cu foam. The entire procedure was conducted using ultrasonicated solution of pyrrole in DI water with the ratio of 500 mg (pyrrole) : 20 ml (DI water) under open-air

conditions. These binder free PPy coated Cu foam will be designated as Femto-Cu PPy, in this work.

2.3 Characterization

X-ray diffraction (XRD) analysis was conducted using an X'Pert3 Powder diffractometer from Panalytical over a 2θ range of 10° to 80° at room temperature, whereas Fourier transform infrared (FTIR) spectra were acquired using a Shimadzu IRTracer-100 spectrometer equipped with a single reflection attenuated total reflection (ATR) accessory. Detailed morphological and elemental characterization was also performed using a TESCAN VEGA 3 LMU scanning electron microscope (SEM), equipped with an INCAx-act energy dispersive spectroscopy (EDS) detector from Oxford Instruments. A CHI 660E electrochemical workstation from CH Instruments Inc. was used for electrochemical measurements. The measurements were carried out in a three-electrode configuration with a 3 M KOH electrolyte, where the Femto-Cu PPy foams served as the working electrode, platinum (Pt) wire as the counter electrode, and Hg/HgO as the reference electrode. Equations S(1) and S(2) were used to calculate the areal (specific capacitance) capacitance (C_{sp}) in F/cm².

Electrochemical calculations

Equation (S1) measured the areal-specific capacitance (C_{sp}) in F/cm² to investigate the charge storage capability *via* CV analysis.

$$C_{sp} = \frac{\int IdV}{2sA\Delta V} \quad (S1)$$

Where, $\int IdV$ = area under the curve (CV curve), s = scan rate (V/s), ΔV = potential window (V) and A = active area of studied electrode (cm²). From GCD curves the C_{sp} values in F/cm² calculated through equation (S2)

$$C_{sp} = \frac{I \Delta t}{A \Delta V} \quad (S2)$$

Where I = applying current (mA), Δt = discharge time (s), ΔV = potential window (V) and A = active area of studied electrode (cm²).

Power law (Equation S3) or Lindstrom's method [3], which correlates current (i) with scan rate (v) was used to quantify or determine the b-values.

$$i = av^b \quad (S3)$$

Where, i and v denote measured current and scan rate, respectively. Whereas the parameters 'a' and 'b' correspond to intercept and slope of the plot log (i) vs. log (v).

Further, for a more detailed study, we utilized Trasattis's method [4] (equation S4) to dissect the total stored charge into capacitive and diffusion-controlled contributions from the plots of 1/Qs vs. \sqrt{v} (scan rate) and Qs vs. $1/\sqrt{v}$ (scan rate) (Potential window is 0.6 V and Qs = specific capacitance, Csp)

$$Q_t = Q_{cap} + Q_{diff} \quad (S4)$$

Where, Q_t is total charge storage capacity (capacitance), Q_{cap} is capacitive mechanisms (surface-controlled capacitance) and Q_{diff} is diffusion-controlled processes (diffusion-controlled capacitance).

To determine the charge storage contribution, we applied the following modified power law or Dunn's method [5] equation S5.

$$\frac{iV}{v^{0.5}} = K_1 v^{0.5} + K_2 \quad (S5)$$

Where, (iV) is the response current having values at current peak (i) and applied voltage window (V) and v is the scan rate. K_1 and K_2 are the slope and intercepts of the line after plotting graph between $\frac{iV}{v^{0.5}}$ and $v^{0.5}$ [6, 7]

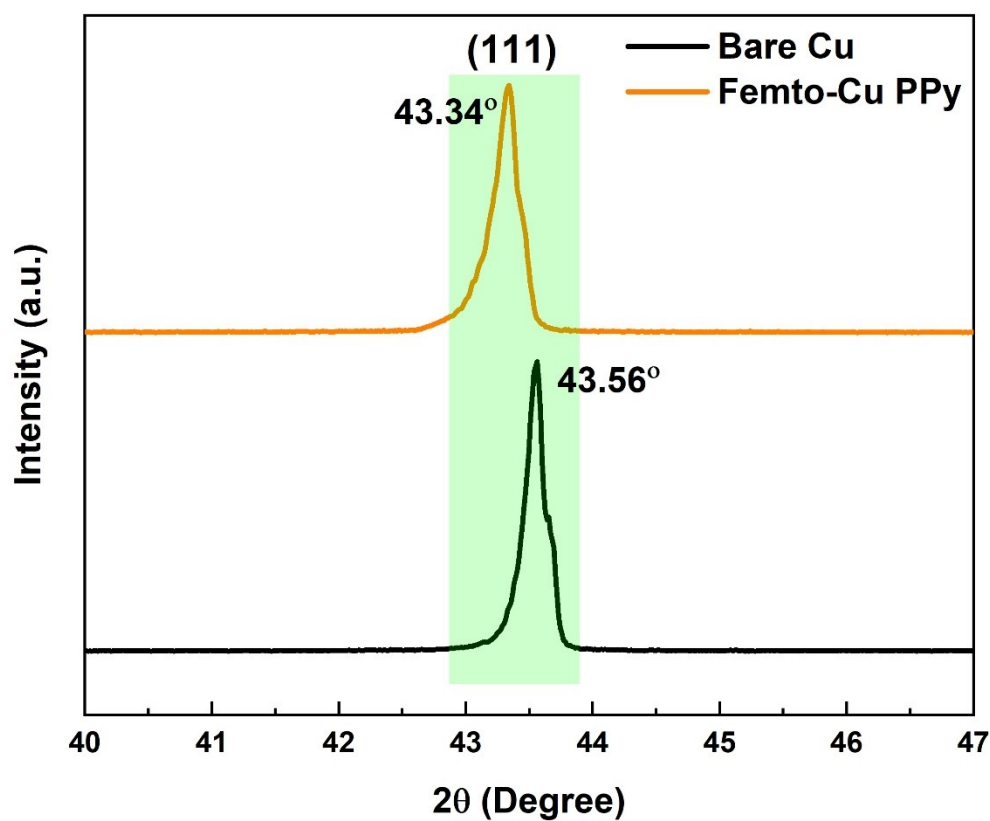


Fig. S1 Enlarged XRD spectra of (111) plane

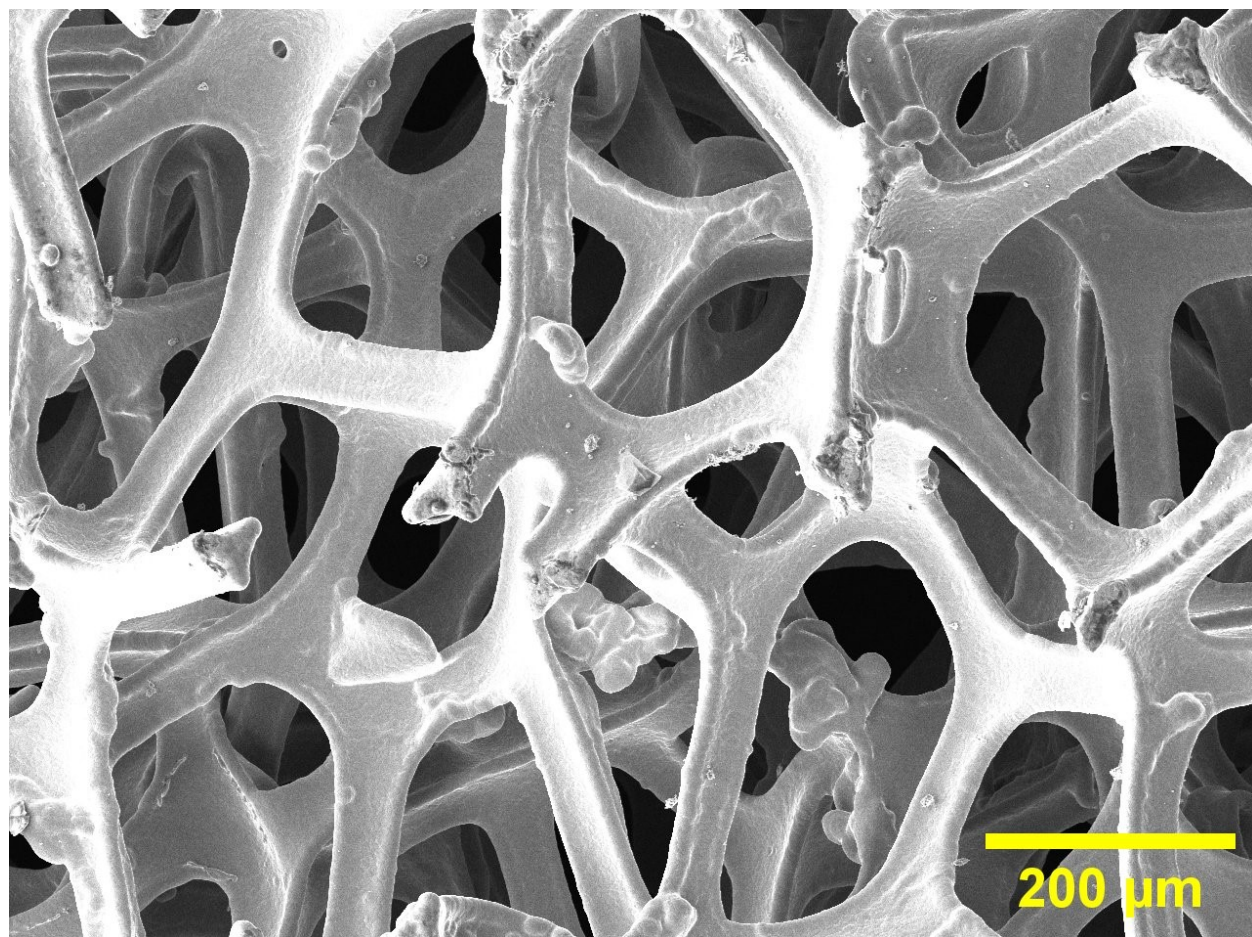


Fig. S2 SEM of bare Cu foam

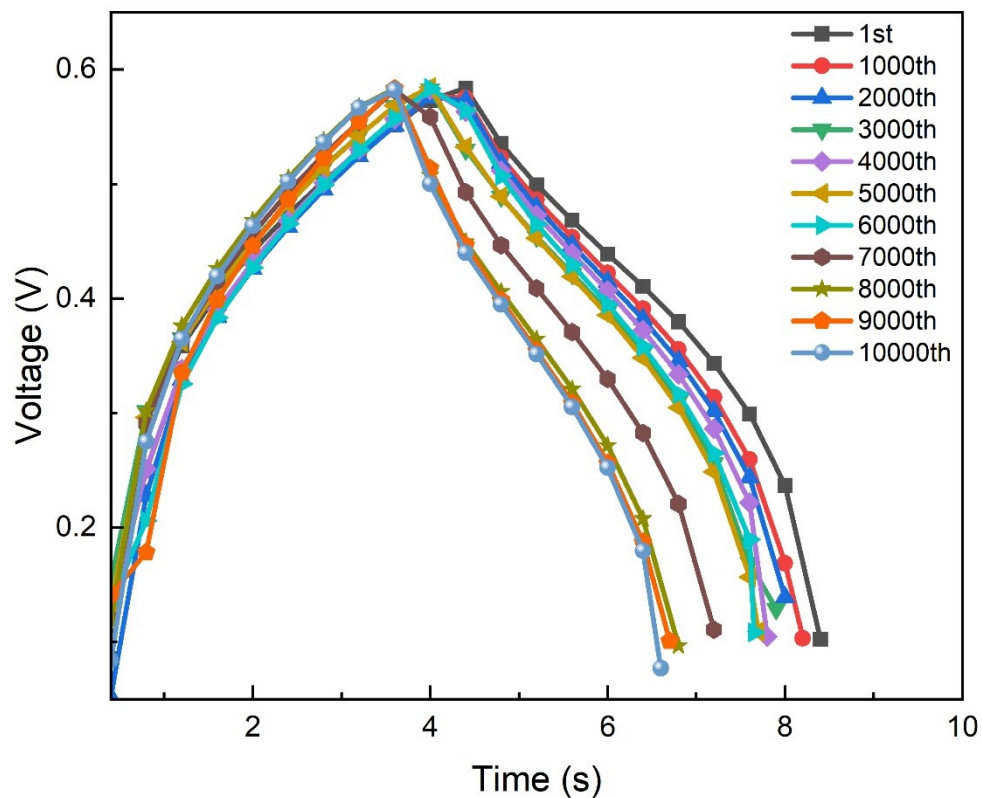


Fig. S3 GCD cyclic stability curves of Femto-Cu PPy at 10 mA/cm² current density

Table S1. Trasattis's method utilized to calculate the specific capacitance values from the plots of $1/Q_s$ vs. $\sqrt{\text{scan rate}}$ and Q_s vs. $1/\sqrt{\text{scan rate}}$

Q_t (mF/cm ²)	Q_{cap} (mF/cm ²)	Q_{diff} (mF/cm ²)
121.07	58.42	62.65

Table S2. Comparison of electrochemical properties of femtosecond laser-structured materials prepared under different conditions.

Current collector	Atmosphere	Electrolyte	Current density (mA×cm ⁻²)	C _{sp} (mF×cm ⁻²)	Ref.
Ni plate	Air	2 M KOH	1.0	92.40	[8]
Ni foam	DI Water	3 M KOH	1.0	138.91	[2]
Porous carbon @ Polyimide (PI) sheets	Air	--- H ₂ SO ₄	0.1	22.40	[9]
1T MoS ₂ @ PI coated platinum	Air	0.1 M H ₂ SO ₄	1.0	4.20	[10]
rGO/RuO ₂ @ polyethylene terephthalate (PET) film	Air	0.1 M H ₂ SO ₄	0.2	7.01	[11]
Graphene @ fallen leaves	Air	--- H ₂ SO ₄	0.03	35.32	[12]
MnO/ Graphene @ wood	Air	1 M Na ₂ SO ₄	1.0	45.00	[13]
MoS ₂ @ gold coated Si wafer	Air	1 M NaOH	0.022	4.88	[14]
rGO @ glass	Air	1 M H ₂ SO ₄	5.0	2.14	[15]
Polypyrrole @ Cu foam	Pyrrole in DI water	3 M KOH	0.5	148.5	This work

References

1. Maqsood, M.F., et al., *Femtosecond Laser-Structured Nickel Foams in Different Atmospheres as Current Collectors for Supercapacitor Applications*. ACS Applied Energy Materials, 2024.
2. Maqsood, M.F., et al., *Boosting the charge storage capability of Ni foams via femtosecond laser structuring in different solvents*. Materials Chemistry and Physics, 2025. **333**: p. 130306.
3. Lindström, H., et al., *Li⁺ ion insertion in TiO₂ (anatase). 2. Voltammetry on nanoporous films*. The Journal of Physical Chemistry B, 1997. **101**(39): p. 7717-7722.
4. Ardizzone, S., G. Fregonara, and S. Trasatti, "Inner" and "outer" active surface of RuO₂ electrodes. Electrochimica Acta, 1990. **35**(1): p. 263-267.
5. Wang, J., et al., *Pseudocapacitive contributions to electrochemical energy storage in TiO₂ (anatase) nanoparticles*. The Journal of Physical Chemistry C, 2007. **111**(40): p. 14925-14931.
6. Latif, U., et al., *Binder free heteroatom-doped graphene oxide as high energy density electrodes for supercapacitor applications*. International Journal of Energy Research, 2022. **46**(7): p. 9643-9666.
7. Pholaupphon, W., et al., *Guidelines for supercapacitor electrochemical analysis: A comprehensive review of methodologies for finding charge storage mechanisms*. Journal of Energy Storage, 2024. **98**: p. 112833.
8. Wang, S., et al., *In situ synthesis of NiO@ Ni micro/nanostructures as supercapacitor electrodes based on femtosecond laser adjusted electrochemical anodization*. Applied Surface Science, 2021. **541**: p. 148216.
9. Wang, S., et al., *High-performance stacked in-plane supercapacitors and supercapacitor array fabricated by femtosecond laser 3D direct writing on polyimide sheets*. Electrochimica Acta, 2017. **241**: p. 153-161.
10. Xu, C., et al., *Miniaturized high-performance metallic 1T-Phase MoS₂ micro-supercapacitors fabricated by temporally shaped femtosecond pulses*. Nano Energy, 2020. **67**: p. 104260.
11. Wang, L., et al., *Femtosecond laser induced one-step nanopatterning and preparation of rGO/RuO₂ electrodes for high-performance micro-supercapacitors*. Journal of Electroanalytical Chemistry, 2022. **919**: p. 116501.
12. Le, T.S.D., et al., *Green flexible graphene–inorganic-hybrid micro-supercapacitors made of fallen leaves enabled by ultrafast laser pulses*. Advanced Functional Materials, 2022. **32**(20): p. 2107768.
13. Kim, Y.-R., et al., *Green supercapacitor patterned by synthesizing MnO/laser-induced-graphene hetero-nanostructures on wood via femtosecond laser pulses*. Biochar, 2024. **6**(1): p. 36.
14. Cao, L., et al., *Direct laser-patterned micro-supercapacitors from paintable MoS₂ films*. small, 2013. **9**(17): p. 2905-2910.
15. Shen, D., et al., *Scalable high-performance ultraminiature graphene micro-supercapacitors by a hybrid technique combining direct writing and controllable microdroplet transfer*. ACS Applied Materials & Interfaces, 2018. **10**(6): p. 5404-5412.